Proceedings of the
44th IEEE Conference on Decision and Control, and
the European Control Conference 2005
Seville, Spain, December 12-15, 2005

Modeling of Intracranial Pressure-temperature Dynamics and Its Application to Brain Hypothermia Treatment

Lu Gaohua, *Non-Member*, and Hidenori Kimura, *Member, IEEE*

***Abstract*—Brain hypothermia treatment (BHT) is efficient in decompressing the intracranial hypertension in neurosurgery. However, BHT is still difficult and ineffective since quantitative relationship between decompression and brain hypothermia is unclear. The aim of this paper is to develop a theoretical model integrating the hemodynamics and the thermodynamics to quantitatively predict transient responses of the elevated intracranial pressure (ICP) to ambient cooling. The model consists of a lumped-parameter compartmental representation of the body and is based on two temperature-dependence mechanisms of metabolism and vascular water filtration. The model is verified by comparing the simulation results to population-averaged data and clinical evidences of BHT. The hypothermic decompression is linearly approximated by a transfer function comprising a gain of about 4.9 mmHg/°C, a dead time of about 1.0 h and a time constant of about 9.8 h. Using these quantitative data, a feedback control of elevated ICP is implemented in a simulated intracranial hypertension of vasogenic brain edema. Simulation results suggest the possibility of automatic control of the elevated ICP in BHT.**

I. Introduction

CONTROL of increased intracranial pressure (ICP) remains an important challenge in neurosurgical practice. Many methods, such as head elevation, diuretics, hyperventilation, cerebral spinal fluid (CSF) drainage, decompressive craniotomy are established for the treatment of raised ICP. As another strategy of decompressing the elevated ICP, brain hypothermia treatment (BHT) has been used successfully for patients suffering from severe head injuries [1]–[4]. For example, in Germany, BHTs were carried out for 39% of patients after traumatic brain injury, about half of which were aimed at control of refractory intracranial hypertension [5].

Relieving brain edema, decreasing cerebral metabolic rate and other multifactorial chemical and/or physical processes are qualitatively considered as the possible mechanisms of hypothermic decompression in clinical studies [1]–[4]. However, the quantitative relationship between ICP and body temperature is still unclear. Up to now, no theoretical study has been carried out on the intracranial pressure and temperature dynamics, and no quantitative guideline has been provided for medical staffs to cool patients efficiently in order to achieve an optimal management of the elevated ICP.

Manuscript received March 2, 2005.

Bio-Mimetic Control Research Center of RIKEN (the Institute of Physical and Chemical Research), Nagoya 463-0003, Japan (phone: 81-52-736-5361; fax: 81-52-736-5362; e-mail: lu@bmc.riken.jp, kimura@bmc.riken.jp).

The aim of this paper is to construct a mathematical model that incorporates the intracranial pressure and temperature dynamics to predict the transient responses of elevated ICP to ambient cooling through computer simulation. Two mechanisms of temperature dependence of metabolism and capillary filtration in tissue are first introduced into the mathematical model to describe the hypothermic effect on physiological functions. The model is verified by comparing various simulation results with existing data and clinical evidences of BHT. The time course of elevated ICP in response to unit step cooling is quantitatively analysed using the simulated intracranial hypertension of vasogenic brain edema and a feedback regulator of the ambient cooling temperature is constructed to control the elevated ICP of a simulated patient at a normal level. The latter opens up a door to automatic regulation of elevated ICP in BHT.

II. Model Description

A. Main Assumptions

Modeling is based on the following basic assumptions:

1). The patient is modeled as a passive system. It is justified by the clinical fact that a general anesthesia is invariably carried out to block the active nervous and hormonal regulations of circulation and metabolism.

2). Model consists of six parallel segments, i.e. the cranial, the cardiocirculatory, the pulmonary, the visceral, the muscular, and the residual segment or 13 compartments (Fig. 1). Two mechanical pumps of constant pressure increments are introduced to represent the heart pumping effects.

3). Lumped parameters are assumed in each compartment. Hydrostatic pressure and temperature of the CSF compartment represent ICP and brain temperature.

4). The muscular segment holds a temperature-adjustable environment corresponding to cooling apparatus of BHT, while the other segments are all thermally insulated from the ambience. Water and heat loss by respiration are negligible.

5). Metabolic water and heat, which are produced only in the mass compartments, depend on the corresponding temperature of mass compartment. At the same time, vascular water filtration is also temperature dependent.

6). Secretion of CSF from the choroid plexuses is considered to be temperature dependent and assumed to be unaffected by pressure such as the cerebral perfusion pressure, ICP or osmotic pressure.

0-7803-9568-9/05/$20.00 ©2005 IEEE

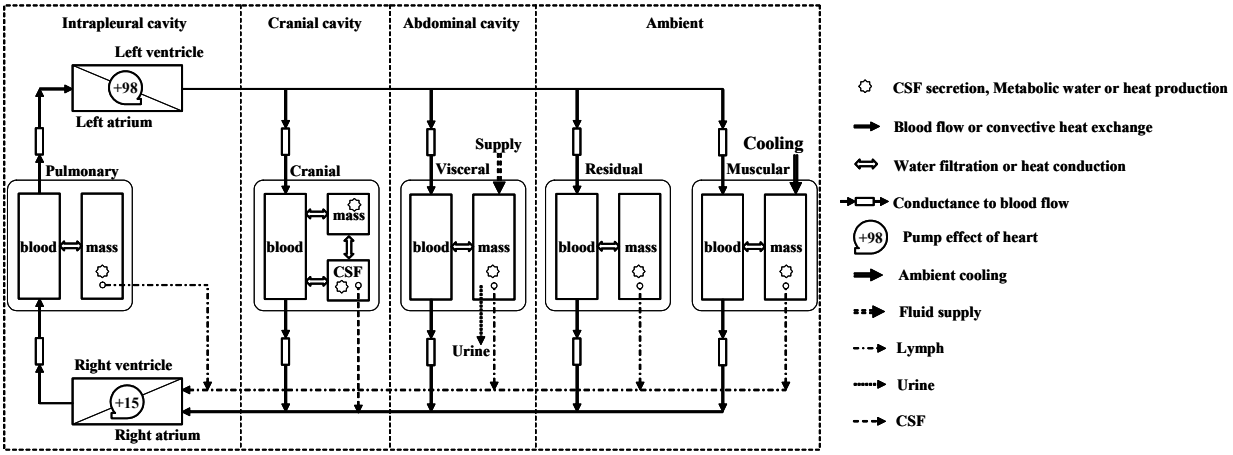

Fig. 1. Compartmental model of the hemodynamics and thermodynamics

B. Model of Hemodynamics and Thermodynamics

The hydrostatic pressures and temperatures in the cranial segment are modeled in detail below. The other portions of the model are constructed similarly. Various symbols are summarized in Table I.

For the CSF compartment,

$$C_{csf}\frac{dP_{csf}}{dt}=W^{crani}_{mass-csf}+W^{crani}_{blood-csf}+M_{csf}-L_{csf}, \tag{1}$$

$$\rho_{csf}c_{csf}V_{csf}\frac{dT_{csf}}{dt}=w^{crani}_{mass-csf}-l_{csf}, \tag{2}$$

for the brain mass compartment,

$$C^{crani}_{mass}\frac{dP^{crani}_{mass}}{dt}=W^{crani}_{blood-mass}-W^{crani}_{mass-csf}+M^{crani}_{mass}, \tag{3}$$

$$\rho^{crani}_{mass}c^{crani}_{mass}V^{crani}_{mass}\frac{dT^{crani}_{mass}}{dt}=w^{crani}_{blood-mass}-w^{crani}_{mass-csf}+m^{crani}_{mass}, \tag{4}$$

and for the cerebral blood compartment,

$$C^{crani}_{blood}\frac{dP^{crani}_{blood}}{dt}=W^{crani}_{artery}-W^{crani}_{vein}-W^{crani}_{blood-mass}-W^{crani}_{blood-csf}, \tag{5}$$

$$\rho^{crani}_{blood}c^{crani}_{blood}V^{crani}_{blood}\frac{dT^{crani}_{blood}}{dt}=w^{crani}_{artery}-w^{crani}_{vein}-w^{crani}_{blood-mass}, \tag{6}$$

where equation (1), (3) and (5) are derived by invoking conservation of mass within each compartment and considering CSF secretion or metabolic water production as a water source. In contrast, equation (2), (4) and (6) are based on conservation of energy within each compartment, while metabolic heat production is considered as a heat source.

Various terms of water or blood flows and heat flows on the right hand sides of equations (1)-(6) are given as follows:

$$W^{crani}_{mass-csf}=K^{crani}_{mass-csf}[(P^{crani}_{mass}-P_{csf})-\sigma(\pi^{crani}_{mass}-\pi_{csf})], \tag{7}$$

$$W^{crani}_{blood-csf}=K^{crani}_{blood-csf}[(P^{crani}_{blood}-P_{csf})-\sigma(\pi^{crani}_{blood}-\pi_{csf})], \tag{8}$$

$$W^{crani}_{blood-mass}=K^{crani}_{blood-mass}[(P^{crani}_{blood}-P^{crani}_{mass})-\sigma(\pi^{crani}_{blood}-\pi^{crani}_{mass})], \tag{9}$$

$$W^{crani}_{artery}=(P_{artery}-P^{crani}_{blood})/R^{crani}_{artery}, \tag{10}$$

$$W^{crani}_{vein}=(P^{crani}_{blood}-P_{vein})/R^{crani}_{vein}, \tag{11}$$

$$w^{crani}_{mass-csf}=k^{crani}_{mass-csf}(T^{crani}_{mass}-T_{csf}), \tag{12}$$

$$w^{crani}_{blood-mass}=k^{crani}_{blood-mass}(T^{crani}_{blood}-T^{crani}_{mass}), \tag{13}$$

$$l_{csf}=\rho_{csf}c_{csf}L_{csf}(T_{csf}-T_{vein}), \tag{14}$$

$$w^{crani}_{artery}=\rho_{blood}c_{blood}W^{crani}_{artery}(T_{artery}-T^{crani}_{blood}), \tag{15}$$

$$w^{crani}_{vein}=\rho_{blood}c_{blood}W^{crani}_{vein}(T^{crani}_{blood}-T_{vein}), \tag{16}$$

where, formulae (7)-(9) represent the water filtrations among the adjacent three compartments in the cranial segment. π is apparent total osmotic pressure value and is constant within each compartment. The reflection coefficient σ is assumed to be 1.0. Formulae (10) and (11) are based on the hydrodynamics of cerebral blood compartment. On the other hand, formulae (12) and (13) describe conductive heat transfers between the adjacent compartments while formulae (14)-(16) describe convective heat transfers.

On account of the temperature-dependence mechanisms, *van't Hoff's equation* and *Arrhenius' law* are introduced to describe the secretion of CSF, the metabolic water or heat production and water permeability.

$$M_{csf}=M_{0csf}Q_{10}^{\frac{T_{csf}-T_{0csf}}{10}}, \tag{17}$$

$$M^{crani}_{mass}=M^{crani}_{0mass}Q_{10}^{\frac{T^{crani}_{mass}-T^{crani}_{0mass}}{10}}, \tag{18}$$

$$m^{crani}_{mass}=m^{crani}_{0mass}Q_{10}^{\frac{T^{crani}_{mass}-T^{crani}_{0mass}}{10}}, \tag{19}$$

$$K^{crani}_{mass-csf}=K^{crani}_{0mass-csf}e^{\frac{E}{1.987}(\frac{1}{273.15+T^{crani}_{0mass}}-\frac{1}{273.15+T^{crani}_{mass}})}, \tag{20}$$

$$K^{crani}_{blood-csf}=K^{crani}_{0blood-csf}e^{\frac{E}{1.987}(\frac{1}{273.15+T^{crani}_{0blood}}-\frac{1}{273.15+T^{crani}_{blood}})}, \tag{21}$$

$$K^{crani}_{blood-mass}=K^{crani}_{0blood-mass}e^{\frac{E}{1.987}(\frac{1}{273.15+T^{crani}_{0blood}}-\frac{1}{273.15+T^{crani}_{blood}})}. \tag{22}$$

Furthermore, compliance of the CSF compartment in equation (1) depends on ICP, as the following formula shows,

$$C_{csf}=\frac{1}{rP_{csf}}, \tag{23}$$

where *r* denotes the elastance coefficient.

For each of the other ten compartments, two differential equations describing hydrostatic pressure and temperature are available, similarly based on the conservation of mass or energy. Taken altogether, the entire model is mathematically described by 26 differential equations.

TABLE I. PARAMETERS CHARACTERIZING THE HEMODYNAMICS AND THERMODYNAMICS

Segment (superscript)	Compartment (subscript)	$V^{(a)}$ (ml)	$\rho^{(a)}$ (g/ml)	$c^{(a)}$ (J/g/°C)	C (ml/mmHg)	$M^{(b)}$ (x10^{-3}ml/s)	$m^{(a)}$ (W)	$L^{(b)}$ (x10^{-3}ml/s)	$q^{(b)}$ (ml/s)	$\pi^{(b)}$ (mmHg)	$R^{(\#)}$ (mmHgs/ml)	$K^{(b)}$ (ml/s/mmHg)	$k^{(¥)}$ (W/°C)	$T_0^{(*)}$ (°C)	$P_0^{(*)}$ (mmHg)	$P_0^{(!!)}$ (mmHg)
Cranial (crani)	CSF (csf)	150	1.0	3.85	ICP-dependent[d,f]	3.858	0	5.787	0	5443		1.285×10^{-4} (mass-CSF)[$]	0.277 (mass-CSF)	37.1	+10	+20.6
	Brain mass (mass)	1374	1.08	3.85	30.503[c]	0.463	14.37	0	0	5423		2.093×10^{-4} (blood-mass)[$]	14.85 (blood-mass)	37.2	+5	+11.9
	Capillary blood (blood)	6	1.059	3.85	0.031[d]	0	0	0	10.833	5443	6.277 2.954	4.186×10^{-8} (blood-CSF)[$]	0 (blood-CSF)	36.2	+32	+31.9
Pulmonary (pulmo)	Lung mass (mass)	1669	0.56	3.52	37.05[e]	0.046	0.61	1.604	0	5429		1.558×10^{-3}	168.0	36.0	-8	-8.1
	Capillary blood (blood)	70	1.059	3.85	0.347[d]	0	0	0	83.333	5443	0.06 0.096			36.0	+7	+6.9
Visceral (visce)	Visceral mass (mass)	4905	1.0[c]	3.7[c]	108.891[e]	-5.178	27.55	5.15	0	5435		3.26	48.92	36.7	-2.7	-2.8
	Capillary blood (blood)	20	1.059	3.85	0.101[d]	0	0	0	35.833	5443	2.308 0.483			36.1	+17.3	+17.2
Muscular (muscl)	Muscular mass (mass)	27668	1.085	3.8	614.23[e]	0.695	18.93	15.695	0	5435		50.03×10^{-3}	300.31	35.4	-3	-3.1
	Capillary blood (blood)	125	1.059	3.85	0.621[d]	0	0	0	17.5	5443	4.726 0.989			35.6	+17.3	+17.2
Residual (resid)	Residual mass (mass)	22023	1.107	2.0	488.911[e]	0.116	16.64	12.273	0	5435		40.525×10^{-3}	243.28	36.2	-3	-3.1
	Capillary blood (blood)	101	1.059	3.85	0.503[d]	0	0	0	19.167	5443	4.315 0.903			36.1	+17.3	+17.2
Cardio-circulatory (heart)	Arterial part (artery)	1129	1.059	3.85	2.5[b]	0	0	0	0	5443				36.0	+100	+99.9
	Venous part (vein)	3609	1.059	3.85	50.0[b]	0	0	0	0	5443				36.0	0	-0.1

t time; T temperature; T_0 temperature in steady state; P hydrostatic pressure; P_0 hydrostatic pressure in steady state; V volume; ρ density; c specific heat; C compliance; M metabolic water production; M_0 metabolic water production at T_0; m metabolic heat production; m_0 metabolic heat production at T_0; L lymphatic flow; l heat flow due to lymphatic flow; q distribution of cardiac output; π apparent total osmotic pressure; R vascular resistance; r elastance coefficient of CSF, 0.11ml^{-1}; K vascular water filtration coefficient; K_0 vascular filtration coefficient at T_0; k vascular conductive heat transfer coefficient; σ reflection coefficient of 1.0; Q_{10} van't Hoff's quotient of 2.8; E Arrhenius activation energy of 7cal/mol; W blood or water flow between two compartments; w heat exchange between two compartments; h cooling coefficient of hypothermic blanket, 8W/m^2/°C. # estimated value based on total peripheral resistance of systemic circulation is of 1.0 mmHgs/ml. The two data are for the resistances between the capillary blood compartment and the arterial and venous part of the cardiocirculatory segment; $ estimated values based on pressure balance among 3 compartments in cranial segment; ¥ estimated values based on convective coefficient of 6 W/m^2/°C; * estimated values of pressure or temperature in steady state; !! estimated values of pressure for the intracranial hypertension in steady state;
a Werner and Buse 1988; b Guyton 2001; c Fiala et al. 1999; d Ursino and Magosso 2000; e Lakin et al. 2003; f Marmarou et al. 1978;

C. Parameter Assignments and Model Computation

Certain values of a healthy, such as the vascular resistances, the compliances, the filtration coefficients, the CSF secretion, the distribution of metabolic or lymphatic water production, the distribution of metabolic heat production, and the initial values of pressure and temperature in steady state have to be either known from other studies, extrapolated or estimated based on current knowledge. The results are shown in Table I.

Obviously, nonlinearities occur in this model. These are multiplicative terms of temperature difference and pressure difference in the thermodynamics, the nonlinear *van't Hoff's equation* and *Arrhenius' law*, and the pressure dependence of the CSF compliance. Furthermore, the ambient cooling, as an input of the hemodynamic and thermodynamic systems, should be kept within the temperature bound of clinical and/or physiological availability. However, computation of this model is done through four-order Runge-Kutta.

D. Explication of Hypothermic Decompression

Physically, therapeutic hypothermia decreases the intracranial temperatures of the thermodynamics. Subsequently, CSF secretion is cooled down according to formula (17), and water filtrations from the adjacent two compartments to the CSF compartment are also depressed, as described by equation (7) and (8) and formula (20) and (21) of the hemodynamics. Therefore, the first three terms on the right hand side of equation (1) are decreased, while the last term is almost unaffected by pressure or temperature. It is why hypothermic decompression of the elevated ICP is realized in the mathematical model.

III. VERIFICATION OF MODEL

The mathematical model is verified by comparing the simulation results with the clinical experience or with the general knowledge reported in the literature.

A. Characteristics of Thermodynamics

The time course of brain temperature response to a unit step cooling from 30 °C to 29 °C is computed (Fig. 2).

Generally, the temporal curve of brain temperature can be considered as the result of a linear process with transfer function of $2.0e^{-0.6s}/(9.2s+1)$, where s denotes Laplace operator. Namely, brain temperature responding to ambient cooling is characterized by a time constant of 9.2 h, a dead time of 0.6 h, and a gain of 2 °C/°C. All of these characteristics are comparable with the clinical experience or data and the existing knowledge of the thermodynamics.

First, the simulated time constant of 9.2 h is consistent with the clinical experience, since it often takes several hours under clinical conditions to introduce hypothermia into the patient's body. For example, Schwab, *et al.* spent little more than 12 h to cool their patients to the target hypothermia [12], while 3-11 h was experienced by Jian and his colleagues [13].

Although a gap exists between the mathematical model and the actual patient, and the cooling strategies applied to clinical practice are evidently different among individual patients and different from the unit step cooling used in this simulation, the simulated time constant of several hours is roughly consistent with the temporal order of BHT induction.

Second, provided that the patient's body is approximated by a lumped weight with an ambient temperature $T_{cooling}$, the

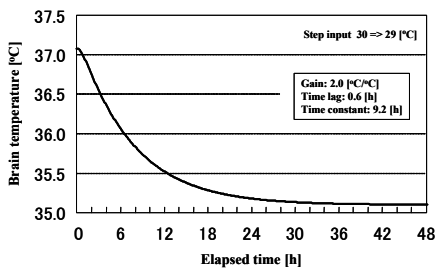

Fig. 2. Unit step response of brain temperature.

governing equation of its representative temperature T will be given as follows:

$$cM\frac{dT}{dt} = -hA(T - T_{cooling}) + Q, \quad (24)$$

where the weight M = 67 kg, the specific heat c = 3.8x10^3 J/kg/°C, the outer surface A =1.8 m^2, and the cooling coefficient h = 8 W/m^2/°C. The metabolic heat production Q depends on the representative temperature T, as described by *van't Hoff's equation* of Q_{10} = 2.8.

From equation (24), the representative temperature in steady state can be numerically calculated as follows: T = 35.4 °C when $T_{cooling}$ = 30 °C, and T = 33.4 °C when $T_{cooling}$ = 29 °C. Therefore, the gain is 2 °C/°C, which is the same as that simulated 2 °C/°C in Fig. 2.

Third, the simulated dead time of 0.6 h is consistent with the existing knowledge reported in the literature. That is, datum of 0.5 h has been cited by Givoni and Goldman [14] in characterizing the dead time of body temperature in response to an ambient cooling.

Based on these agreements, we can conclude that the model is effective in describing the dynamic response of brain temperature of a real patient to an ambient cooling.

B. Characteristics of Hemodynamics

Dynamic response of ICP is computed for the case that a bolus of fluid is inserted into the CSF compartment at a constant infusion rate. This computation corresponds to the infusion test carried out in clinical practice.

A bolus injection of total volume of 2 ml with a constant infusion rate of 0.66 ml/s is applied to the model (Fig. 3). In response to 2-ml infusion between 10 and 13 s, ICP exhibits an initial peak followed by a monotonic return toward baseline. Maximum ICP increase of about 3.4 mmHg occurs at the time of infusion end.

The simulation results are fully consistent with the clinical experience. That is, in a classic nonlinear analysis of the CSF system and ICP dynamics, Marmarou *et al.* [11] has shown that if a bolus of fluid is added to the intracranial cavity, ICP will change transiently from its initial value, followed by gradual return to the predisturbance level. Moreover, with the same infusion maneuver of 2 ml during 3 s, Ursino and Lodi [15] obtained a similar result in their mathematical model of the interaction between ICP and cerebral hemodynamics, provided that the autoregulation was impaired. The similarity of these two results is also considered as a support of the validity of the mathematical model in describing the hemodynamics of a sedated patient in BHT.

IV. Applications of Model

A. Modeling of Intracranial Hypertension

In order to simulate a pathophysiological state of elevated ICP, an assumption of damaged blood-brain barrier (BBB) function can be made. For example, a 100-fold increased filtration in BBB was assumed by Rapoport [16] in his hydraulic model of vasogenic brain edema while a cerebral permeability increase by a factor of 1000 above the normal value was implied for a more permeable cerebral capillary.

In this model, a characteristic state of ICP over 20 mmHg is simulated by increasing capillary filtrations of blood-brain and -CSF barriers 1000 times as large as those of the normal. As a result, a patient model of intracranial hypertension responsible for vasogenic brain edema is theoretically produced in the model, by mathematically adjusting only one of its physiological parameters, i.e. the barrier permeability, without concomitant changes in other parameters. In this case, a new set of values of hydrostatic pressure of the hemodynamics is estimated for the simulated patient in steady state. The result is shown in Table I by marker of !!.

In the following theoretical analysis, the raised ICP will be considered as the control target while the simulated patient model of brain edema is used to replace the actual patient with intracranial hypertension that requires decompression.

B. Response of Intracranial Hypertension to Step Cooling

Time course of the elevated ICP in the simulated model of brain edema in response to the step decrease of the ambient temperature from 30 °C to 27 °C is simulated (Fig. 4).

Cooling of 3 °C is efficient in decreasing the elevated ICP from more than 20 mmHg to about 6 mmHg and furthermore, most of the decompression occurs within 10 h. This shows that, the elevated ICP responses to the ambient cooling strongly (decreasing from >20 mmHg to <6.4 mmHg), but slowly (maximal rate of 1.5 mmHg/h at 2.6 h). The latter is probably due to the inertia of the intracranial pressure-temperature dynamics. This result reflects the usefulness, as well as the hardness, of hypothermic decompression, in agreement with the clinical experience.

Nonlinearity is observed, i.e. decompression effect from a reduction in an ambient temperature of 3 °C (from 30 °C to 27 °C) is not effective as three times as that of 1 °C reduction (from 30 °C to 29 °C, data not shown). However, for the sake

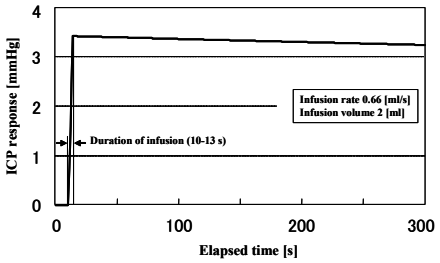

Fig. 3. Simulated infusion test.

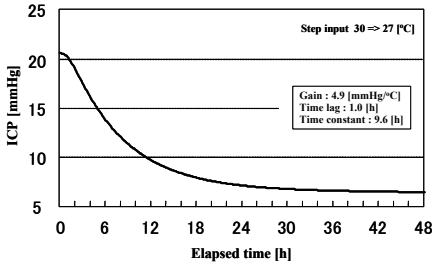

Fig. 4. Step response of intracranial hypotension.

of clinical applicability, linear characteristic approximation is available. The temporal course of the elevated ICP in response to step cooling may be considered as the result of an integrated process of dead time and first-order delay. The transfer function $G(s)$ from the ambient cooling temperature to the elevated ICP is given by

$$G(s) = e^{-s\lambda} \frac{\kappa}{\tau s + 1}, \tag{25}$$

where τ, λ and κ denote time constant, dead time and gain, respectively.

As shown in Fig. 4, these characteristic parameters are estimated in the simulated intracranial hypertension of vasogenic brain edema. That is, the elevated ICP response to changes in the ambient cooling temperature is characterized by gain of about 4.9 mmHg/°C, dead time of about 1.0 h and time constant of about 9.8 h.

C. Feedback Control of Intracranial Hypertension

Using the characteristic approximation of (25), a PID feedback regulator is designed in order to reduce the elevated ICP first and then to maintain ICP at a normal level by regulating the ambient cooling temperature. Cooling temperature $T_{cooling}$ is estimated as

$$T_{cooling} = K_P(e + \frac{1}{T_I}\int edt + T_D \frac{de}{dt}), \tag{26}$$

where e denotes the difference between the reference ICP and the estimated ICP. The latter is the output of a simulated patient model of brain edema when the estimated cooling temperature $T_{cooling}$ at the last sampling time is applied to the model. The reference ICP is set at 9.9 mmHg. The controller parameters are adjusted according to the following formulas, based on the optimal tuning of Chien-Hrones-Reswick [17].

$$K_P = 0.6\tau/\lambda\kappa\,,\ T_I = 0.3\tau\,, T_D = 0.5\lambda\,. \tag{27}$$

Therefore, K_P = 1.2 °C/mmHg, T_I = 3.0 h, and T_D = 0.5 h.

Raised ICP is lowered to 10 mmHg during the regulated cooling (Fig. 5). In detail, in response to the regulated cooling temperature, the ICP, with an initial value of more than 20 mmHg, decreases to the normal range at a maximal rate of about 4.0 mmHg/h at 1.7 h. The target ICP is achieved within 4.5 h. After an overshoot of 0.5 mmHg at 5.9 h, ICP is maintained with a difference of as little as 0.16 mmHg from the reference ICP at the end of 24 h simulation. That is, an overshoot of about 5% and a control error within 1.6% occur in the controlled ICP, although the classical formula (27) is designed for the optimal tuning without overshoot. It is presumed that both of them are due to the linear approximation of the nonlinear intracranial pressure-temperature dynamics.

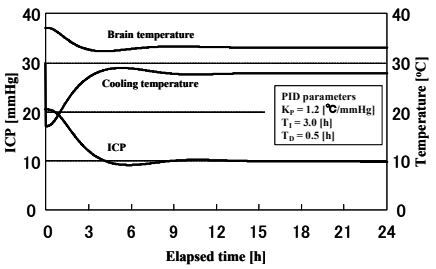

Fig. 5. PID feedback control of intracranial hypotension.

As shown in Fig. 5, the estimated cooling temperature is temporally smooth, namely, no larger variation in the cooling temperature is required to realize a constant control of the elevated ICP. On the other hand, with the estimated cooling temperature, brain temperature of the model decreases to about 32 °C in a similar time scale as the elevated ICP does. This result implies the consistency of the management of brain temperature and that of elevated ICP in BHT.

In clinical practice, PID feedback control of elevated ICP may be manually realized by the medical staff based on their experience and/or by trial and error. However, as shown in this simulation, it is possible to implement an automatic control of intracranial hypertension when approximated characteristics of the intracranial pressure-temperature dynamics are used for various patients in the intensive care unit. Such an automatic control would allow the medical staff to effectively manage the elevated ICP through therapeutic hypothermia.

V. Discussion

In patients with severe brain injury, elevated intracranial pressure (ICP) means poor prognosis and high mortality. Brain hypothermia treatment (BHT) has been verified to be effective for patients with refractory ICP elevation, in whom all other conventional therapeutic options failed in decompression [1]. Hypothermia, however, has to be carried out by the medical staff's experience to control the elevated ICP in clinical practice. An efficient ICP-oriented BHT is impossible unless a quantitative guideline on control of the elevated ICP coupled with temperature management is provided for the medical staff.

This paper aims to attack this problem from the viewpoint of control by theoretically modeling and simulating. On the basis of qualitative knowledge of hypothermic decompression, two temperature-dependence mechanisms of metabolism and vascular water filtration have been introduced in the mathematical model. To the best of our knowledge, this is the only model in which the mechanisms of temperature dependence are included as a key for combining the hemodynamics and the thermodynamics.

Concerning the hypothermic decompression, a gain of about 4.9 mmHg/°C, a dead time of about 1.0 h and a time constant of about 9.8 h are first estimated as quantitative data for the medical staff, by using the linear approximation of the time course of elevated ICP in response to step cooling applied to the simulated patient model of vasogenic brain edema. Similar conclusions of the linear approximation are obtained in other simulated intracranial hypertensions, such as in swelling, in hydrocephalus or in hematoma (data not shown). Hence, these three characteristic data can reasonably be adopted as a criterion of hypothermic decompression. With knowledge of these characteristic parameters, the elevated ICP response to a known ambient cooling can be

predicted, or inversely, in order to depress an elevated ICP in a clinical patient to a normal range, the required cooling procedure can be suggested.

It is worth pointing out that most of physical and physiological parameters in this model are based on literature. The model simulation results show transient responses in elevated ICP to unit step cooling or bolus injection of volume agree well with the population-averaged data or the existing clinical knowledge. As shown in the simulation of feedback control of the elevated ICP, the estimated cooling temperature is physically available and clinically applicable. Although discrepancy between the theoretical model and the actual patient may exist, the results achieved in this paper can be applied to the clinical practice, for example, providing characteristic parameters useful in diagnosis and assessing possible changes induced by BHT.

Apart from the two temperature-dependence mechanisms of metabolism and vascular water filtration, there are other mechanisms responding to hypothermic decompression. For example, hypothermia may prevent BBB dysfunction by decreasing permeability of serum albumin into the brain tissue through the injured BBB. And another possible mechanism is the hypothermic depressions of cerebral circulation and cardiac pumping function. For the sake of simplicity, these mechanisms are neglected in this model.

Furthermore, there are some limitations in the present model that need to be addressed.

(1) The present model is restricted to simulating a passive system. The addition of partially inhibited active regulation mechanisms in the future would allow medical staffs to extend this model to more direct clinical applications.

(2) The present model has excluded the possible influence of the respiration system. The relational effect of regulated respiratory therapy on elevated ICP control is another future research topic, as hyperventilation physiologically lowers elevated ICP by inducing hypocapnia vasoconstriction.

(3) Apart from effort to improve the theoretical model, a robust adaptive control mechanism may be an option in dealing with the uncertainness of individual variation caused by medical treatment and/or patient recovery.

VI. Conclusion

A mathematical model of the intracranial pressure-temperature dynamics has been constructed to quantitatively analyse the hypothermic decompression in BHT. The model has been verified by comparing the transient responses in brain temperature to ambient cooling and the transient responses of ICP to a bolus injection with the population-averaged data and the general clinical knowledge. It has been shown that, with time constant of about 9.8 h and dead time of about 1.0 h, the elevated ICP may decrease about 4.9 mmHg in response to a 1 °C decrease in ambient cooling temperature. A PID feedback control of elevated ICP is realized by automatically regulating the ambient cooling temperature on the basis of the estimated characteristic parameters.

The mathematical model allows the medical staff to probe this integrated dynamics theoretically, often in much greater detail than is possible in experimental studies, and can therefore help them to find a novel strategy to manage elevated ICP and a clinical application of an ICP-oriented BHT. For this purpose, more future theoretical work needs to be done to improve the mathematical model and to improve the control mechanism used in the management of the pathophysiological process in a clinical patient.

References

[1] K. H. Polderman, "Application of therapeutic hypothermia in the ICU: opportunities and pitfalls of a promising treatment modality. Part 1: Indications and evidence," *Intensive Care Med.*, vol. 30, no. 4, pp. 556–575, Apr. 2004.

[2] K. H. Polderman, R. Tjong Tjin Joe, S. M. Peerdeman, W. P. Vandertop, and A. R. J. Girbes, "Effect of therapeutic hypothermia on intracranial pressure and outcome in patients with severe head injury," Intensive Care Med., vol. 28, no. 11, pp. 1563–1573, Nov. 2002.

[3] N. Hayashi, "The clinical issue and effectiveness of brain hypothermia treatment for severely brain-injured patients," in *Brain hypothermia*, N. Hayashi, Ed. Tokyo: Springer-Verlag, 2000, pp. 121–151.

[4] N. Hayashi, "Clinic management". in *Brain hypothermia treatment*, N. Hayashi and D. W. Dietrich, Ed. Tokyo: Springer-Verlag, pp. 37–317.

[5] S. Himmelseher and C. Werner, "Therapeutic hypothermia after traumatic brain injury or subarachnoid hemorrhage. Current practices of German anaesthesia departments in intensive care," *Anaesthesist*, vol. 53, no. 12, pp. 1168–1176, Dec. 2004.

[6] J. Werner and M. Buse, "Temperature profiles with respect to inhomogeneity and geometry of the human body," *J. Appl. Physiol.*, vol. 65, no. 3, 1110–1118, Sep. 1988.

[7] A. C. Guyton, *Textbook of medical physiology*, Pennsylvania: W.B. Saunders Company, 2001.

[8] D. Fiala, K. J. Lomas, and M. Stohrer, "A computer model of human thermoregulation for a wide range of environmental conditions: the passive system," *J. Appl. Physiol.*, vol. 87, no. 5, pp. 1957–1972, Nov. 1999.

[9] M. Ursino and E. Magosso, "Acute cardiovascular response to isocapnic hypoxia. I. A mathematical model," *Am. J. Physiol. Heart. Circ. Physiol.*, vol. 279, no. 1, pp. H149–H165, Jul. 2000.

[10] W. D. Lakin, S. A. Stevens, B. L. Tranmer, and P. L. Penar, "A whole-body mathematical model for intracranial pressure dynamics," *J. Math. Biol.*, vol. 46, no. 4, pp. 347–383, Apr. 2003.

[11] A. Marmarou, K. Shulman, and R. M. Rosende, "A nonlinear analysis of the cerebrospinal fluid system and intracranial pressure dynamics," *J. Neurosurg.*, vol. 48, no. 3, pp. 332–344, Mar. 1978.

[12] S. Schwab, D. Georgiadis, J. Berrouschot, P. D. Schellinger, C. Graffagnino, and S. A. Mayer, "Feasibility and safety of moderate hypothermia after massive hemispheric infarction," *Stroke*, vol. 32, no.9, pp. 2033–2035, Sep. 2001.

[13] S. Jian, Q. Yongming, C. Zhihua, and C. Yan, "Feasibility and safety of moderate hypothermia after acute ischemic stroke," *Int. J. Dev. Neurosci.*, vol. 21, no.6, pp. 353–356, Oct. 2003.

[14] B. Givoni and R. F. Goldman, "Predicting rectal temperature response to work, environment, and clothing," *J Appl. Physiol.*, vol. 32, no. 6, pp. 812-822, Jun. 1972.

[15] M. Ursino and C. A. Lodi, "A simple mathematical model of the interaction between intracranial pressure and cerebral hemodynamics," *J. Appl. Physiol.*, vol. 82, no. 4, pp. 1256–1269, Apr. 1997.

[16] S. I. Rapoport, "A mathematical model for vasogenic brain edema," *J. Theor. Biol.*, vol. 74, no. 3, pp. 439–467, Oct. 1978.

[17] K. L. Chien, J. A. Hrones, and J. B. Reswick, "On the automatic tuning of generalized passive systems," *Trans. ASME*, vol. 74, pp. 175–185, Feb. 1952.